UCRL-11897

University of California

Ernest O. Lawrence Radiation Laboratory

CLIMB OF IMPERFECT DISLOCATIONS IN ALUMINUM

Berkeley, California

DISCLAIMER

Research and Development

UCRL - 11897

UNIVERSITY OF CALIFORNIA

Lawrence Radiation Laboratory
Berkeley, California

AEC Contract No. W-7405-eng-48

CLIMB OF IMPERFECT DISLOCATIONS IN ALUMINUM

Nathapet Durai Raghavan

(M. S. Thesis)

January 1965

Contents

CLIMB OF IMPERFECT DISLOCATIONS IN ALUMINUM

Nathapet Durai Raghavan

Inorganic Materials Research Division, Lawrence Radiation Laboratory
and Department of Mineral Technology, College of Engineering,
University of California, Berkeley, California

ABSTRACT

Climb of imperfect dislocations in aluminum of 99.999 purity has been studied by transmission electron microscopy. Annealing at different temperatures of the electron microscope specimens was carried out in a furnace, the specimen being periodically returned to the electron microscope for observation of selected dislocation loops. Friedel's theory of dislocation climb has been applied to the climb of imperfect loops to explain the observed rates of decrease in loop diameter with annealing time at various temperatures. The experiments give 130 ergs/cm^2 as the stacking fault energy of aluminum.

I. INTRODUCTION

When a metal is quenched from a high temperature, a large supersaturation of vacancies is frozen in. Thus, when pure aluminum is quenched from 600 to 0°C, a supersaturation of the order of 10^{-4} is obtained. It is now well established that, on aging, these vacancies cluster in a way that eventually leads to the formation of dislocation loops.[1] Observations in quenched and aged pure fcc materials by transmission electron microscopy have led to the identification of three types of defect structures.

1. Imperfect dislocation loops with Burger's vectors $\frac{a}{3}\langle 111\rangle$ that surround an area of intrinsic stacking fault on the {111} planes: Though the mechanism of loop formation is not yet clearly understood it is believed that vacancy discs on {111} planes collapse to form this type of dislocation loop. These loops have been observed in high purity aluminum[2-4] and in alloys.[5,6]

2. Stacking fault tetrahedra with stair-rod dislocations at each edge: These have been observed in metals of low stacking fault energy. Hirsch and Silcox[7] first reported tyis type of defect in quenched gold.

3. Perfect prismatic loops: In metals of high stacking fault energy like aluminum, an imperfect loop may be converted to a perfect loop of Burger's vector $\frac{a}{2}\langle 110\rangle$ by a shear of $1/6\langle 121\rangle$ in the plane of the fault. The type of defect was first predicted by Kuhlman-Wilsdorf[8] and subsequently observed by Hirsch et al.[9]

The relative energies of the three types of defects that could be formed from a given number of vacancies can be estimated if the stacking

fault energy of the metal is known. They are given approximately by:[10]

$$E_L = \frac{Ga^2 \ell}{4\pi(1-\sigma)} \ln \frac{\ell}{r_o} + \frac{\sqrt{3}}{4} \ell^2 \gamma$$

$$E_T = \frac{Ga^2 \ell}{12\pi(1-\sigma)} \ln \frac{\ell}{r_o} + \sqrt{3}\, \ell^2 \gamma$$

$$E_P = \frac{Ga^2 \ell}{2.4(1-\sigma)} \ln \frac{2\sqrt{2}\ell}{a}$$

where E_L, E_T and E_P are the energies of a triangular imperfect loop, a tetrahedron and a triangular perfect loop, respectively, each having side ℓ, G the shear modulus, a the unit cell dimension, r_o the dislocation core radius, σ Poisson's ratio and γ the stacking rault energy. It follows then that the perfect loop always has the lowest energy above an upper critical size, and the tetrahedron is always favored below a lower critical size.[11,12] Between these two values of ℓ the imperfect loop is stable.

In the absence of a vacancy supersaturation, all of these defects become unstable. When the temperature is raised to a range that permits formation and migration of vacancies, they tend to shrink in size by loss of vacancies to surfaces or to other dislocations having larger radius of curvature. In this way, Silcox and Whelan[13] found that perfect prismatic loops begin to shrink in aluminum when the temperature is about 170°C and that the rate of shrinkage increases with temperature. They interpreted their results in terms of the jog theory of dislocation climb due to Friedel[14] and obtained a value of 1.3 eV for the activation energy for self-diffusion in aluminum, which was in good agreement with previous data.

Yoshida et al.[4] studied the effect of annealing on stacking fault loops by bulk annealing zone refined quenched aluminum specimens at various temperatures. They found that the loops shrink without loss of the stacking fault even though they are well above the size at which transformation to a perfect loop decreases the loop energy.

For imperfect loops the driving force for shrinkage comes not only from line tension of the dislocation, but also from the stacking fault. For large loops the latter is by far the more important. Therefore, a measurement of the temperature dependence of the shrinkage rate for large imperfect loops can give a measure of stacking fault energy.

The accurate determination of the stacking fault energy of aluminum has been difficult by other methods because of its large value. Theoretical calculations by Saada,[11] based on the relative energies of an imperfect loop and a perfect loop and the difficulty of nucleating a Shockley partial in an imperfect loop, have given the upper and lower limits of the stacking fault energy of aluminum as 350 ergs/cm^2 and 140 ergs/cm^2, respectively. Saada[15] and Thornton et al.[16] have reviewed the general methods of measurement of stacking fault energy. Briefly, the following have been the important approaches.

1. It is assumed that the stacking fault energy equals twice the twin boundary energy γ_{TB}. γ_{TB} can be determined by measuring the stress necessary to create a twin and relating it to a general theory of twinning or more directly by measuring the dihedral angle at the intersection of a twin and a free surface or a grain boundary. Using the latter method Fullman[17] found γ_{TB} for aluminum to be 100 ergs/cm^2. However, it appears that the simple assumption that the stacking fault energy equals $2\gamma_{TB}$

may not be valid.[16]

2. A direct method of determining the stacking fault energy is to measure the width of the stacking fault ribbon between the partials of a split dislocation. This is, however, possible only for crystals with γ less than 5 ergs/cm^2 because, otherwise, the partials are too close together to be resolved in the electron microscope.

3. Another direct method consists of measuring the radii of curvature of extended nodes.[18, 19] Unfortunately, the method is limited to solids with $\gamma/Gb \lesssim 2 \times 10^{-3}$. This limitation excludes most of the nominally pure fcc metals.

4. An indirect method of comparing stacking fault energies of different metals has been proposed by Seeger.[20] The thermally activated process of cross slip occurring at the onset of stage III of work hardening in crystals of fcc materials involves the formation of constrictions in the dislocation ribbons and, therefore, depends on the stacking fault energy of the metal. In Seeger's model for cross slip the leading dislocation in a piled-up group is constricted along a critical length before transferring to the cross slip plane. This analysis of τ_{III} (the stress at the onset of stage III) should enable the stacking fault energy to be calculated. Unfortunately, in many cases the stacking fault energies determined by Seeger's analysis do not agree with values determined from electron microscope observations od dissociated nodes[16] and the nature of disagreement is such as to throw serious doubt on the applicability of the method.

The purpose of these experiments was therefore twofold: (a) to study the climb of the imperfect loops by transmission electron micros-

copy, and (b) to try to make a better estimate of the stacking fault energy of aluminum.

II. EXPERIMENTAL PROCEDURES

1. Specimen Preparation.

Polycrystalline aluminum of purity 99.999% was rolled into thin sheets of 25μ thickness. Specimens 1" square were cut off the strip and annealed at 645°C in air for 24 hours. This treatment gives a highly preferred [100] orientation with a large grain size (~ 0.8 mm) and a low dislocation density.

2. Quenching.

The specimen was kept at 540°C for one hour in the quenching furnace and then quenched into oil at room temperature. The low quenching temperature and the relatively low quenching rate[21] both tend to give large loops. The specimen was then aged at room temperature to allow the vacancies to diffuse through the lattice and cluster to form loops.

3. Preparation of Thin Foils.

Quenched and aged specimens were electro-polished at -10 to -20°C using an electrolyte of the following composition

Perchloric Acid (70%) - 110 cc

Ethyl Alcohol (95%) - 480 cc

A stainless steel container served as the cathode. The operating voltage was 15-25 volts and the current density 0.15 - 0.2 amp/cm^2. A modified window technique was employed to produce thin foils. Near the end of the thinning process, the current was alternately switched on and off causing small flakes suitable for transmission microscopy to separate from the thin edges and fall to the bottom of the beaker. The flakes were copiously washed with 100% alcohol to get a clean surface,

free from any contamination.

4. Microscopy.

A Siemens Elmiskop I electron microscope operated at 100 KV was used to examine the specimens. The specimens were mounted between two 75 mesh copper grids. The condenser aperture used for 400μ in diameter and the effective beam current less than 5μA.

Shrinkage of dislocation loops can be made to take place while under observation in the microscope by utilizing a heating stage. However, there are some disadvantages if quantitative results are desired. One of these is the lack of precision in knowing the temperature of the specimen; ±5°C is probably the best that can be expected with currently available stages. Further, there is often a movement of the specimen accompanying a change in temperature which changes the tilt and, therefore, the diffraction contrast conditions. Another disadvantage is that a series of pictures can be taken at only one area.

Because of these considerations it was decided to anneal the specimens externally in a furnace. The following procedure was adopted.

(a) Several regions were photographed in which large stacking fault loops, well separated from their neighbors, were present.

(b) The specimen holder was removed from the microscope and the specimen holder cap, which contains the specimen sandwiched between two grids, was carefully unscrewed from the body of the holder and threaded onto a screw which was attached to the end of a long wire.

(c) This was introduced into a tube furnace. Argon was passed through the tube at a flow rate just sufficient to maintain a slightly positive pressure. The temperature during the annealing

period was measured to an accuracy of ±1°C.

(d) After annealing for the desired period, the cap was withdrawn to the top of the tube where it was cooled to room temperature in the argon atmosphere.

(e) Then the cap was again fitted to the body of the electron microscope specimen holder and returned to the microscope for a second observation of the same areas. During these observations any shift of the specimen relative to the grids made location of the same areas difficult, if not impossible, when the specimen was returned to the microscope for the next series of pictures.

(f) Annealing times were increased by repeating the above procedure as many as five or six times.

A great advantage in this method is the minimization of the effects due to heating by the electron beam. The temperature the specimen attains in the microscope is dependent upon four factors, viz., (1) operating voltage, (2) thickness of the foil, (3) beam diameter and (4) the beam current. Simple considerations show that the higher the voltage and the smaller the other three factors, the lower the equilibrium temperature of the specimen will be. For the conditions maintained in the present experiments (Kv -100, foil thickness ~ 2500Å, beam diameter - 5μ and beam current < 5μA), it was probably less than 50°C, a temperature at which diffusion is insignificant.

Great care was exercised at each stage so as not to deform the specimen and thus destroy the stacking faults in imperfect loops. When stacking fault loops were converted to perfect loops by stress aided nucleation of a Shockley partial loop in the stacking fault, they

usually moved along their glide cylinders to one of the foil surfaces and thus were lost.

5. Measurement of Loop Size.

Since the foil orientation was invariably [100] and since the loops lie on {111} planes inclined at an angle of 54° 44' to the plane of the foil, the longest diagonal of the loop was taken as a measure of the loop size. Because this diameter lies parallel to the surface of the foil, slight differences of tilt of the specimen relative to the electron beam from one observation to the next do not cause significant errors. However, since the image size depends on $\bar{g}.\bar{b}.s.$, as far as possible, care was taken to keep $\bar{g}.s$ of constant sign for all measurements during a particular annealing sequence.

III. RESULTS AND INTERPRETATION

The results are shown in Figures 1-5. Each of these figures show sequences of micrographs taken at successively increasing annealing times at a fixed annealing temperature. Annealing temperatures of 158°C, 168°C, 175°C, 185°C and 190°C, are represented by the five figures. The results clearly show that Frank-sessile loops on annealing in the temperature range 150-200°C frequently shrink without loss of the stacking fault. Those loops that did transform to perfect $\frac{1}{2}\langle 110\rangle$ loops probably nucleated $\frac{1}{6}\langle 112\rangle$ loops in the stacking fault during handling. Large bending stresses could have been produced in the thin foil specimen during removal of the specimen cap from and its return to the specimen holder. The lowest temperature at which imperfect loops were observed to shrink at a noticeable rate was ~158°C (Fig. 1), in contrast to ~170°C, as reported by Whelan[13] for perfect prismatic loops. The rate of shrinkage increased rapidly with increasing temperature. For example, the sequences of micrographs in Fig. 2-4 show that the rates of decrease of radii of loops of about 700Å initial radii were about .42Å, .525Å and 1Å per sec., at 168°C, 175°C and 185°C, respectively. In general, loops which were originally hexagonal became rounder (loop 1, Fig. 1), or irregular in shape (loop 1, Fig. 8), as annealing time increased. Also, all loops both large and small shrank in thin foils which indicates that the foil surfaces were the only important sinks for vacancies. The rate at which imperfect loops decreased in size was almost independent of loop diameter above about .05μ in diameter, but increased with decreasing loop size for smaller loops. The loop

diameters for five of the loops in Fig. 5 have been plotted as a function of time at 190°C in Fig. 6.

The observations suggest that the loops were acting as vacancy sources. An imperfect loop on the (111) plane is a pure edge dislocation. Its extra half plane of atoms lies outside the loop. Therefore, formation of vacancies at the dislocation causes climb toward the loop center. Friedel[14] has considered the climb of dislocations due to vacancy diffusion in terms of the movement of jugs along the dislocation line. The theory gives the following expression for the velocity of a jog, v_j, along a dislocation line:

$$v_j = \frac{Z\, \nu_a\, b}{\sin \psi} \exp\left\{-\frac{(U_f + U_m)}{kT}\right\} \left[\exp \frac{F_c b^2}{kT} - \exp \frac{F_s b^2}{kT}\right] \qquad (1)$$

where $Z \approx 11$ (the atomic coordination number of a jog site at the edge of the extra half plane of an edge dislocation, ν_a is an atomic frequency (of the order of 10^{13}/sec.), ψ is the angle between the Burger's vector $\bar{b}$ and the dislocation line, U_f is the energy of formation of a vacancy, U_m is the activation energy for the migration of a vacancy, $U = U_f + U_m$ is the activation energy for self-diffusion, and F_c and F_s are forces per unit length acting on the dislocation line tending to make it climb. F_c is the force due to an applied stress, the stress field of another dislocation or the stacking fault enclosed by the loop. F_s is the chemical stress due to any deviation of the concentration of vacancies from the equilibrium value at temperature T.

This expression can now be applied to a $\frac{1}{3}\langle 111\rangle$ imperfect loop. Consider a hexagonal loop lying on the (111) plane with a Burger's

vector $\frac{1}{3}$ [111]. For shrinkage of such a loop it is not necessary to nucleate new jogs. Jog sites are already present at each of the corners even if all the six sides are atomically straight. The formation of each vacancy at the dislocation loop results in the elimination of the stacking fault in an area $\approx b^2$. Therefore, the stacking fault exerts a climb force per unit length equal to γ in magnitude.

Besides the stacking fault the line tension due to the curvature of the dislocation also acts to cause climb and hence, will contribute to the magnitude of F_c. For circular loop we can employ the following approximate expression for this force f_c due to line tension:[22,23]

$$f_c = \frac{G\,b}{4\pi(1-\sigma)} \quad \frac{\ln\,(r/b)}{(r/b)} \qquad (2)$$

where the radius of the core has been taken as b and the core energy neglected.

It is assumed that the vacancies are removed fast enough at the surfaces so that no significant supersaturation exists in the neighborhood of the loops. Therefore, F_s can be taken as zero. Such supersaturations do become important in thick specimens[13] or in the presence of large amounts of impurities;[24] large loops then grow at the expense of smaller ones. As an additional precaution against possible errors due to supersaturation effects, only loops that were at least one foil thickness apart from the surrounding loops were used for the calculations. A good estimate of foil thickness was made by means of slip traces that could be made to appear at the end of a series of observations by prolonged exposure of the area to the electron beam.

The average rate of climb of the dislocation is given by

$$v = v_j \, c_j \sin \psi \tag{3}$$

where c_j is the concentration of jogs on the line. c_j will be of the order of ½ if the loop is perfectly circular and can be almost zero if it is perfectly hexagonal. It is assumed that a value of ½ holds for all segments of the loop. For a pure edge dislocation $\sin \psi = 1$. Assuming that $F_s = 0$, the rate of shrinkage will therefore be given by

$$\frac{dr}{dt} = -\tfrac{1}{2} v_j = \tfrac{1}{2} Z \nu_a b \exp \left\{ \frac{-(U_f + U_m)}{kT} \right\} \left[\exp \frac{(\gamma + f_c) b^2}{kT} - 1 \right] \tag{4}$$

Of the two forces, namely, that due to the stacking fault within the loop and that due to the line tension (because of the curvature of the line), the effect of the former is independent of the size of the loop. The line tension term is, however, decisively affected by the radius and shape of the loop. It becomes significant during the initial stage when the loop is changing from a hexagonal shape to a circular one and at the very end when the loop has shrunk to a small size. In between its effect is practically negligible. For instance, assuming γ_{Al} to be 150 ergs/cm^2 and the initial loop size 1000Å in diameter, we find that the line tension contribution is 0.1 γ or greater only during the shrinkage of approximately the first 200Å and last 60Å of the diameter. A rate curve of the shape indicated in Fig. 7 is then predicted.

The experimental results of Fig. 6 show, in excellent agreement with this, that a rapid initial shrinkage of the long diagonal followed by a linear decrease in diameter with annealing time occurs. In those cases where shrinkage was followed to very small diameters (less than

about .05μ), acceleration of the shrinkage rate was observed. The straight line regions of the curves where the effect of line tension was negligible and, hence, the rate of shrinkage almost independent of loop size were used for calculation of the stacking fault energy. For these regions Eq. (4) reduces to

$$\frac{dr}{dt} = \tfrac{1}{2}\, Z\, \nu_a\, b \exp\left\{\frac{-(U_f + U_m)}{kT}\right\}\left[\exp\frac{\gamma b^2}{kT} - 1\right] \qquad (5)$$

Equation (5) suggests three methods for the determination of stacking fault energy. One is the direct substitution of the rate of shrinkage in Eq. (5) to calculate γ. This method is critically dependent on the accurate knowledge of the activation energy for self-diffusion. A variation of 0.1 eV from 1.3 to 1.4 leads to a change in calculated stacking fault energy of from ∿ 130 ergs/cm^2 to ∿ 350 ergs/cm^2. Table I summarizes the results so obtained for three different temperatures. A value of 1.32 eV has been assumed for the energy of formation and migration of a vacancy. This is an average value from previous experimental determinations of the activation energy for self-diffusion in aluminum.[25,26]

The second method is a direct comparison of the rates of shrinkage of imperfect loops, of approximately the same size, at two different temperatures. This method requires extremely accurate temperature measurement during annealing, as well as exact knowledge of the activation energy for self-diffusion. An error of 1°C gives rise to a corresponding error of 50 to 100% in the calculated stacking fault energy. The stacking fault energies obtained by this method were very much scattered and hence are not being reported. Because annealing temperatures were only controlled to ± 1°C in the available annealing

furnace such a large scatter is to be expected.

Finally, the stacking fault energy can be determined by comparing the shrinkage rates of an imperfect loop and a perfect one at the same temperature. This has the advantage of requiring neither an accurate knowledge of U_f and U_m, nor extremely accurate annealing temperature measurement and control. Unfortunately, not many perfect loops were found for study. The results that were obtained from a few loops are presented in Table II.

The values obtained from methods 1 and 3 are seen to be in good agreement with the lower limit for the stacking fault energy of aluminum as estimated by Saada.[10] It is, however, possible that the values are on the lower side of the actual value. Other factors that could cause the slowing down of the rate of shrinkage of a loop may lead to an underestimate of the stacking fault energy. The most important possibility is probably the trapping of impurity atoms along the dislocation line. The tendency for impurity atoms to migrate to cores of dislocations and stacking faults is well recognized. The effect of the presence of an impurity atom is to make the formation of vacancies more difficult at corners of hexagonal loops and also at ordinary jog sites. The activation energy for self-diffusion terms then involves three energies, viz., U_f, U_m and B where U_f is the energy of formation of a vacancy, U_m the energy of migration of a vacancy and B the binding energy of a vacancy to the impurity atom. Such a poisoning of jogs was first proposed by Friedel.[27]

The behavior of loop 1 in Fig. 8 is probably the manifestation of this type of impurity effect. Figure 9 is a magnified schematic drawing of this loop in a sequence of increasing annealing times. In (a)

and (b) the loop has started shrinking by the climb of the edge AB; shrinkage elsewhere is small. After 8 minutes of annealing time overall shrinkage has begun to occur. This could be due to locking of parts of the loop by impurity atoms. More experiments on zone refined aluminum are necessary to establish whether or not the irregular shapes sometimes assumed by shrinking loops were due to impurity poisoning of jogs.

IV. CONCLUSIONS

1. Direct evidence for the climb of imperfect dislocations has been obtained.

2. Friedel's theory of dislocation climb by motion of jogs has been developed to give an expression for the climb rate of imperfect loops and the observed shrinkage has been shown to be in agreement with theory: line tension affects rate significantly only during the initial period when the shape is changed from hexagonal to circular and during the final period when loop size is smaller than about 0.05μ. During the intermediate period shrinkage rate is practically independent of the loop size.

3. The climb rate expression was used to calculate the stacking fault energy of aluminum and a value of $\sim$ 130 ergs/cm^2 obtained using two different methods. It is suggested that this may be an underestimate of the actual value because there were some indications that impurities may have been present in sufficient concentration to influence the results.

ACKNOWLEDGMENTS

The author expresses his deep gratitude to Professor Jack Washburn for his continued interest and encouragement and to Professor Gareth Thomas for his valuable suggestions. This work was supported under the auspices of the U.S. Atomic Energy Commission through the Inorganic Materials Research Division of the Lawrence Radiation Laboratory.

REFERENCES

1. K. Chik, A. Seeger and M. Ruhle, Proc. 5th Int. Congress on Electron Microscopy, Academic Press (1962), p. J-11.

2. R.M.J. Cotterill and R.L. Segall, Phil. Mag., 5, 24 (1960).

3. J.L. Strudel and J. Washburn, Phil. Mag., 9, 491 (1964).

4. S. Yoshida, M. Kiritani and Y. Shimomura, J. Phys. Soc. Japan, 18, 175 (1963).

5. R.B. Nicholson, Report of Int. Conference on Structure and Properties of Thin Films at Bolton Landing, New York (1959), p. 193.

6. K.H. Westmacott, R.S. Barnes, D. Hull and R.E. Smallman, Phil. Mag., 6, 829 (1961)

7. P.B. Hirsch and J. Silcox, Phil. Mag., 4, 72 (1959).

8. D. Kuhlman-Wilsdorf, Phil. Mag., 3, 125 (1958).

9. P.B. Hirsch, J. Silcox, R.E. Smallman, and K.H. Westmacott, Phil. Mag., 3, 897 (1958).

10. G. Thomas and J. Washburn, Rev. Mod. Phys., 35, 992 (1963). See also Lawrence Radiation Laboratory Report No. 10674.

11. G. Saada, J. Phys. Soc., Japan, 18 (III), 41 (1963).

12. G. Czjzek, A. Seeger and S. Mader, Phys. Stat. Sol., 2, 558 (1962).

13. J. Silcox and M.J. Whelan, Phil. Mag., 5, 1 (1960).

14. J. Friedel, Dislocations, Addison-Weley Publishing Co. (1964).

15. G. Saada, Stacking Faults in Crystals, draft for a course at the Prague Conference Summer School (1964).

16. P.R. Thornton, T.E. Mitchell and P.B. Hirsch, Phil. Mag., 7, 1349 (1962).

17. R.L. Fullman, J. Appl. Phys., 22, 448 (1951).

18. M.J. Whelan, Proc. Roy. Soc., A 249, 114 (1958).

19. A. Howie and P.R. Swann, Phil. Mag., 7, 63 (1961).

20. A. Seeger, R. Berner, and H. Wolf, Z. Phys., 155, 247 (1959)

21. G. Das and J. Washburn, "Defects Formed from Excess Vacancies in Aluminum", Phil. Mag., in press.

22. F.C. Frank, Plastic Deformation of Crystalline Solids, ONR (1958), p. 89.

23. H. Franz and E. Kröner, Z. Metallkde, 46, 639 (1953).

24. A. Eikum and G. Thomas, J. Phys. Soc., Japan, 18 (III), 98 (1963).

25. T. Federighi, Phil. Mag., 4, 502 (1959).

26. W. Desorbo and D. Turnbull, Acta Met., 7, 83 (1959).

27. J. Friedel, Dislocations and Mechanical Properties of Crystals, Lake Placid Conference (1956), John Wiley & Sons (1957), p. 346.

FIGURE CAPTIONS

Figures 1-5 and 8 show sequences of same area ((a) in all cases) annealed at various temperatures for increasing times.

Fig. 1 Annealing Temperature 158°C. (b) 4 min., and (c) 8 min.

Fig. 2 Annealing Temperature 168°C. (b) 4 min. (c) 8 min., and (d) 12 min.

Fig. 3 Annealing Temperature 175°C. (b) 4 min. (c) 8 min. (d) 12 min., and (e) 16 min.

Fig. 4 Annealing Temperature 185°C. (b) 3 min., and (c) 6 min.

Fig. 5 Annealing Temperature ∿ 190°C. (b) 4 min. (c) 8 min. (d) 12 min., and (e) 16 min.

Fig. 6 Rate of Shrinkage Curves for Some of the Loops of Fig. 5.

Fig. 7 Predicted Rate Curve for an Imperfect Loop.

Fig. 8 Annealing Temperature ∿ 190°C. Note the Irregular Shrinkage of Loop 1.

Fig. 9 Schematic Drawing of Loop 1 of Fig. 8 in (c) Sequence of Increasing Annealing Times.

Arrows in Fig. 1 - 5 and 8 point at the same group of loops.

TABLE I

Temperature in °K	Rate of Shrinkage Å/sec.		$\exp - \frac{U_f + U_m}{kT} \times 10^{16}$	γ ergs/cm^2	
	Averaged	Highest Observed		i	ii
411	0.32	0.53	8.177	93	126
448	0.525	0.84	14.09	92	122
458	1	1.43	29.7	87	135

TABLE II

Temperature in °K	Rate of Shrinkage Å/ sec.		γ ergs/cm^2
	Imperfect Loop	Perfect Loop*	
448	840	0.07 (~1250Å)	135
458	1.4	.12 (~1250Å)	122
458	1.4	.3 (~ 400Å)	130

*Size of the perfect loop in consideration is given within parantheses.

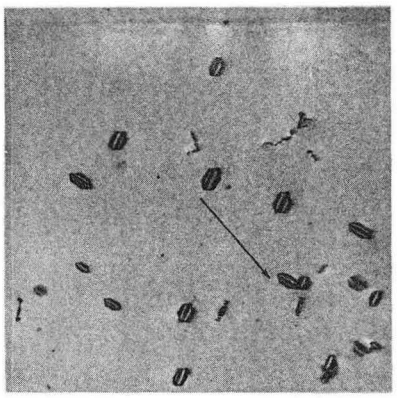

(a)

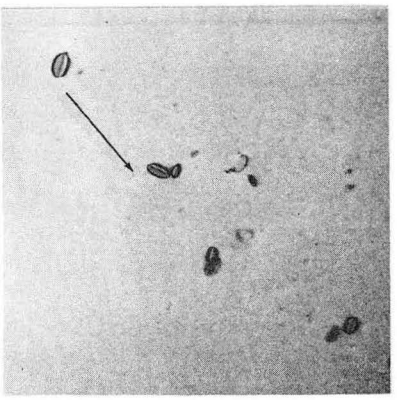

(b)

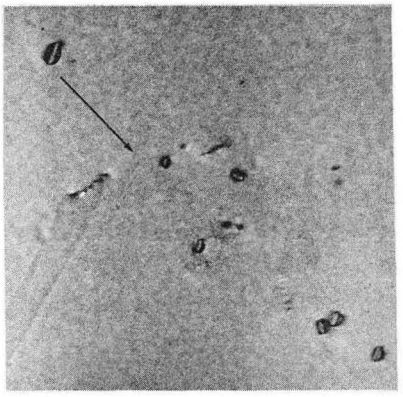

(c)

ZN-4677

Fig. 1

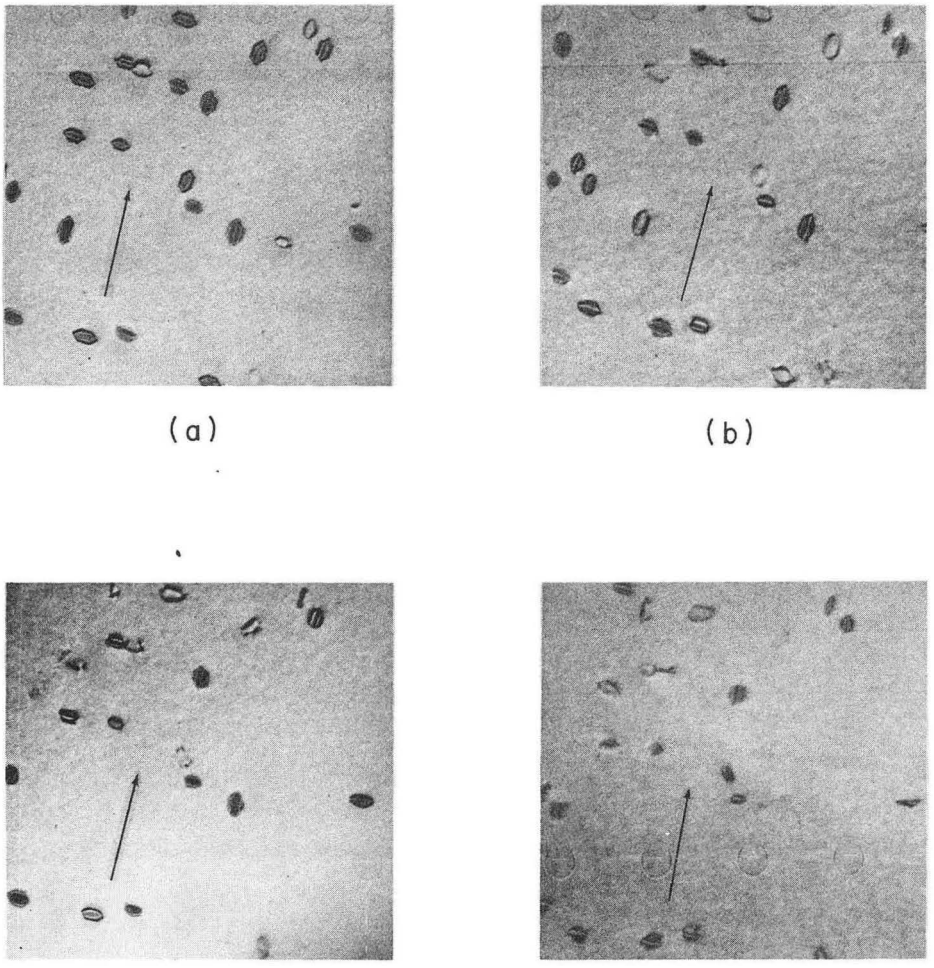

Fig. 2

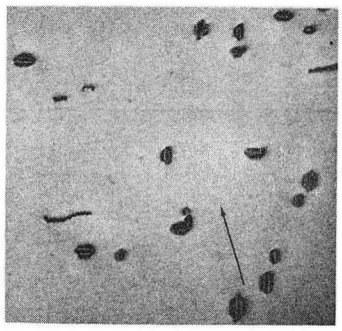

(a)

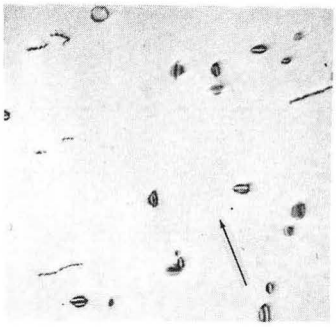

(b)

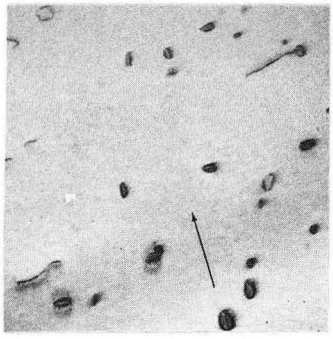

(c)

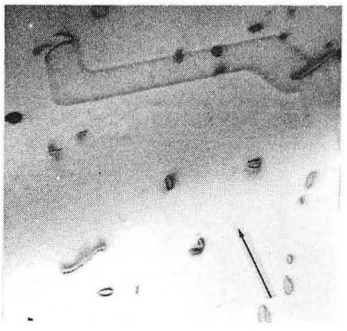

(d)

(e)

ZN-4681

Fig. 3

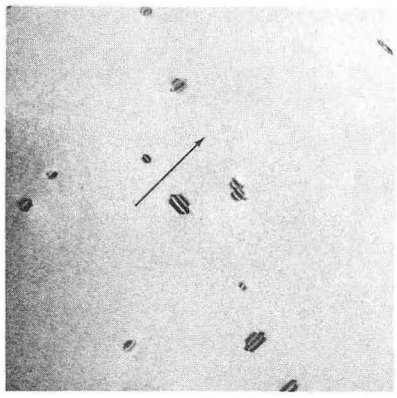

(a)

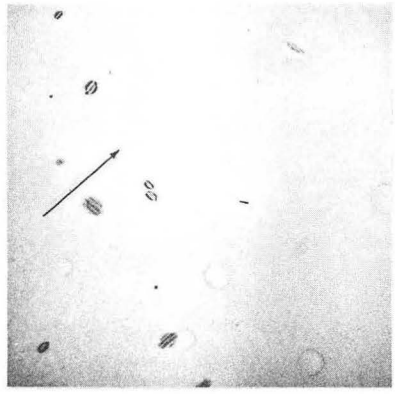

(b)

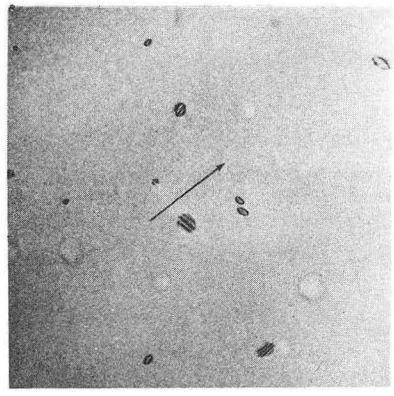

(c)

ZN-4680

Fig. 4

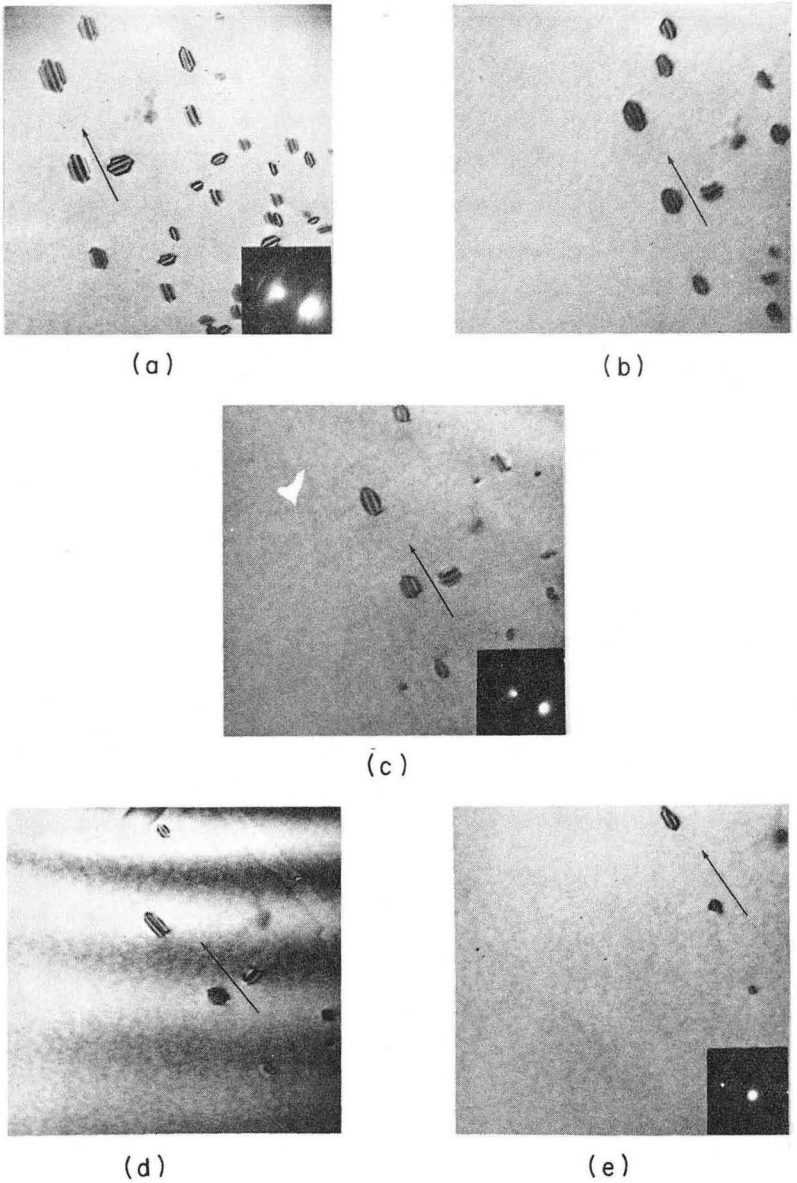

ZN-4679

Fig. 5

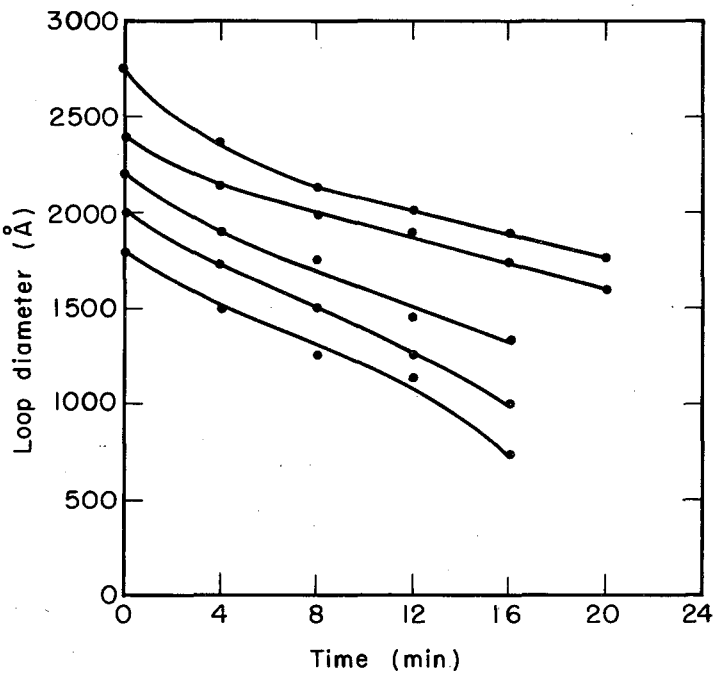
3000
2500
2000
1500
1000
500
0
Loop diameter (Å)
0
4
8
12
16
20
24
Time (min.)
MU-35129

Fig. 6

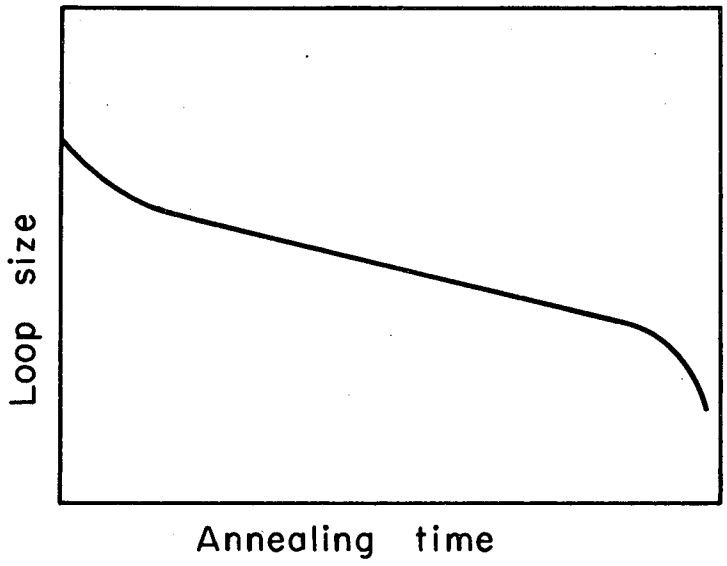

MU-35130

Fig. 7

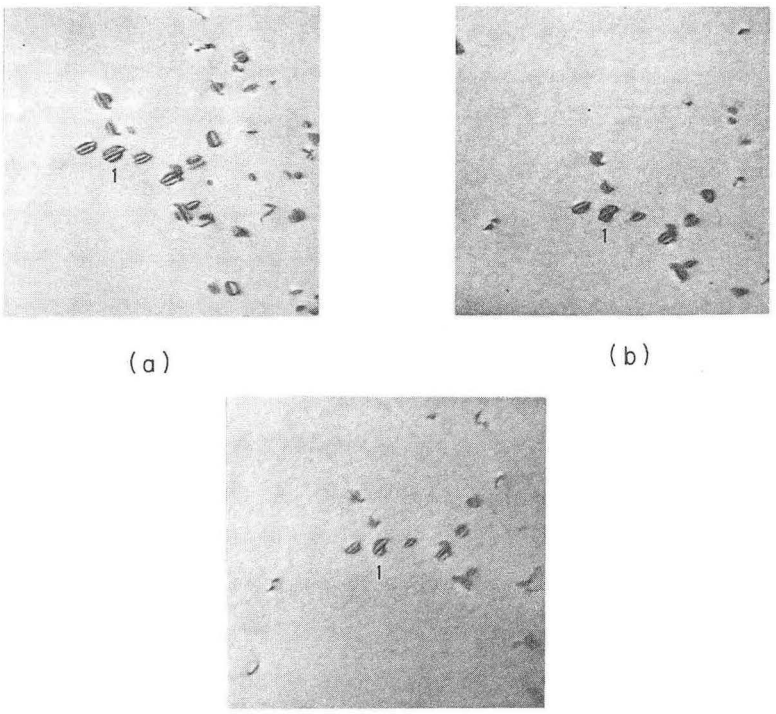

(a) (b)

(c)

(d) (e)

ZN-4678

Fig. 8

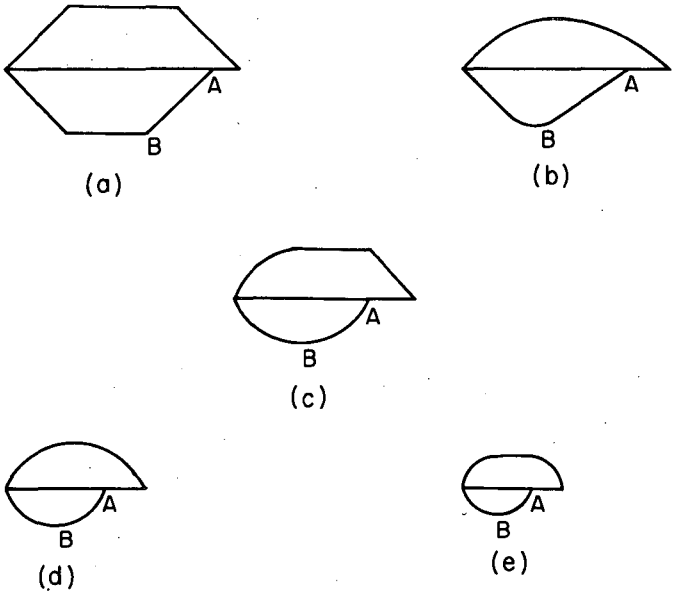

Fig. 9